J. Electrochem. Sci. Eng. **16** (2026) 3644; https://doi.org/10.5599/jese.3644

Open Access : : ISSN 1847-9286
https://pub.iapchem.org/ojs/index.php/JESE

Original scientific paper

Electrocatalytic oxidation and determination of hydrazine at the surface of dioxo-molybdenum(VI) complex-$NiFe_2O_4$ nanoparticle--modified carbon paste electrode

Seamaa Azher Abd-Alhussein[1,✉], Zainab Ayad Wajeeh[2] and Hameed Madlool Mohammed[3]

[1]*Department of Medical Instrumentation Engineering Techniques, College of Engineering, Al-Siraj University College, Al-Fallujah city, Al-Anbar, Iraq*
[2]*Department of Medical Instrumentation Engineering Techniques, College of Engineering, Al-Siraj University College, Al-Fallujah city, Al-Anbar, Iraq*
[3]*Department of Pharmacy, College of Pharmacy, Al-Siraj University College, Al-Fallujah city, Al-Anbar, Iraq*

Corresponding Author: ✉*seamaa.alrubaiei@gmail.com*

Received: July 21, 2026; Accepted: September 7, 2026; Published: October 28, 2026

Abstract

$NiFe_2O_4$ nanoparticles and a dioxo-molybdenum(VI) complex were used to create a modified carbon paste electrode (Mo/NFO/CPE) and investigate the electrocatalytic oxidation of hydrazine (HZN) on its surface. By catalytically reducing the anodic overpotential, the Mo/NFO/CPE significantly improved the kinetics of HZN electro-oxidation. Using a variety of electrochemical techniques, the mechanism of HZN electrochemical behaviour at Mo/NFO/CPE surface was examined. The developed modified electrode demonstrated highly sensitive voltammetric responses for HZN, which makes it ideal for detecting HZN at trace levels. In pH 7.0 buffered solution, a linear dynamic range of 0.1 to 350.0 µM and a detection limit of 0.07 µM were found for HZN.

Keywords: Environmental pollution; nickel ferrite nanoparticles; Mo-based mediator; voltammetric analysis

Introduction

The electrochemical oxidation of hydrazine (HZN) is attractive in direct HZN-based fuel cell (DHFC) technologies, HZN-assisted water splitting, and electrocatalysis in energy conversion [1]. It serves as the anodic reaction in DHFCs, giving these devices compact, high-power sources for specialized and portable applications with quick kinetics and high theoretical energy density [2]. Energy-wise, substituting HZN oxidation at the anode for the sluggish oxygen evolution reaction (OER) greatly

lowers the cell voltage required for hydrogen generation, which lowers energy consumption and increases overall system efficiency [2].

As a result, HZN -assisted water electrolysis presents a viable method for producing hydrogen at low energy costs, particularly when combined with renewable energy sources [3]. However, handling and using HZN poses significant safety issues because of its intrinsic toxicity and environmental concerns [3]. Therefore, accurate and sensitive HZN detection is essential to guarantee safe operations across various energy fields. Although sensitive, traditional detection methods such as chromatographic [4] and spectroscopic [5] approaches often require costly equipment, complex procedures, and time-consuming sample preparation, limiting their use for field analysis or real-time monitoring. In contrast, electrochemical sensing enables real-time environmental monitoring by providing quick, precise detection [6].

Hence, developing devices integrated with both HZN sensing and oxidation functionality would benefit the realization of safe, clean, and renewable energy devices [7]. Ultimately, realizing these advantages in practical devices depends on efficient, selective, and robust electrocatalysts [8]. Thus, the rational design of state-of-the-art electrocatalytic systems remains an active research field, enabling environmentally friendly energy conversion and remediation by HZN oxidation [9].

For detecting various compounds from trace to higher concentrations, electroanalytical methods, particularly voltammetry, offer some additional advantages over more expensive high-performance liquid chromatography and spectroscopic methods, including the ability to measure very small quantities, low cost, good limits of detection, excellent accuracy, and analysis over an extensive linear range in minimum time [10,11]. However, direct analysis of drugs and biomolecules at bare electrodes can cause high overpotential and low sensitivity during analysis [12], driving the design of modified electrodes as state-of-the-art sensors [13].

Because of their many advantages, including straightforward fabrication, low cost, easy surface regeneration, minimal background current and significant miniaturization capability, carbon-paste electrodes (CPEs) are widely acknowledged as one of the most favoured types of working electrodes in electrochemical research [14]. Nevertheless, a significant drawback of bare CPEs is their poor electrochemical performance, mainly due to inadequate electron transport at the electrode-analyte interface [15]. Chemically modified electrodes (CMEs) have been used as a workable solution to this problem [16].

Adding several modifiers has been shown to greatly improve the electrochemical characteristics of CPEs. As a result, these developments expand the use of CPEs in electrochemical sensing and analytical methods, making them a flexible platform for creative study in this field [17,18].

$NiFe_2O_4$ (nickel ferrite) nanostructures are used in biosensors due to their surfaces that can immobilize biomolecules. Bimetallic oxides have attracted attention in bioanalysis and electroanalysis due to their intrinsic mixed-valence property that enhances their activity and conductivity largely. $NiFe_2O_4$ (NFO) has chemical stability and good electrical performance [19]. Moreover, it has a moderate price and is regarded as one kind of magnetic material having relatively strong electrical resistivity among many others, which gives it more application scope in various electrical appliances [20]. Molybdenum- and its derivatives-based mediators are among the most effective mediators [21,22].

According to our search, no study has documented the electroanalytical measurement of HZN utilizing dioxo-molybdenum(VI) complex-$NiFe_2O_4$ nanoparticle-modified CPE (Mo/NFO/CPE). Therefore, in this study, we first discussed the fabrication and appropriateness of a Mo/NFO/CPE as a novel electrode in the determination of HZN. Next, we assessed the Mo/NFO/CPE's analytical performance in HZN quantification in actual samples.

(cc) BY

Experimental

Apparatus and chemicals

All electrochemical experiments were performed on an Autolab potentiostat/galvanostat (PGSTAT 12 N, Netherlands). Platinum wire, Ag/AgCl/KCl and Mo/NFO/CPE were used as the auxiliary, reference and working electrodes.

Double-distilled water was used to freshly make each solution. Analytical-grade HZN and all other reagents were obtained from Merck (Germany). Orthophosphoric acid and its salts in the pH range of 2.0 to 9.0 were used to create buffered solutions (PBS). The dioxo-molybdenum(VI) complex $[MoO_2(L)(CH_3OH)]$ was produced as previously reported in the literature [23].

Synthesis of $NiFe_2O_4$ nanocomposites

The co-precipitation method is used to synthesize $NiFe_2O_4$ nanocomposites. For this purpose, 37.2 g of $NiCl_2{\cdot}6H_2O$ and 406.5 g of $FeCl_3{\cdot}6H_2O$ were dissolved together in 200 mL of water, inside a 500 mL double-necked volumetric flask. The resulting solutions were then heated for 6 hours at 80 °C in an oil bath while maintaining a nitrogen atmosphere. At the same time, the solutions were kept under magnetic stirring so that the initial small nuclei that formed the nanocomposites were well formed and not simply floating around (50 mL of 6 M NaOH was added slowly during this process). After a few minutes, the nuclei responsible for $NiFe_2O_4$ metal nanocomposites began to form, and the formation pathway became clear. The resulting solution was rinsed a few times with distilled water to get rid of the impurities. After that, the obtained product was centrifuged to separate the precipitates that relate to the formation of $NiFe_2O_4$ nanocomposites. Finally, to purify the product and eliminate the leftover impurities inside the structure, the products were put in an oven for 24 hours at 60 °C.

Preparation of the electrode

The Mo/NFO/CPEs were prepared by hand-mixing about 0.02 g of the molybdenum complex with 0.94 g of graphite and 0.04 g of $NiFe_2O_4$. Then, ~0.5 mL of paraffin oil was poured into the mixture. That paste was then filled into the end of a glass tube (geometrical area of 0.09 cm^2). For comparison purposes, molybdenum complex-modified CPE (Mo/CPE) without $NiFe_2O_4$ nanoparticles, $NiFe_2O_4$ nanoparticle carbon paste electrode (NFO/CPE) without molybdenum complex, and unmodified CPE in the absence of both molybdenum complex and $NiFe_2O_4$ nanoparticles were prepared in the same way.

Preparation of real samples

We used a variety of water samples, tap water (from the lab) and urine samples as the actual samples in accordance with the research design. All samples were filtered three times before experiments. Then, different HZN contents were added to the samples, which were then analysed.

Results and discussions

Electrochemical properties of dioxo-molybdenum(VI) complex / $NiFe_2O_4$ nanoparticles modified carbon paste electrode

Electrochemical properties of Mo/NFO/CPE were investigated using cyclic voltammetry (CV) (Figure 1). The insolubility of the molybdenum complex in aqueous environments is one benefit of using it as an electrode modifier. Repeatable, distinct anodic and cathodic peaks with E_{pa} and E_{pc} of 0.325 and 0.230 V were observed.

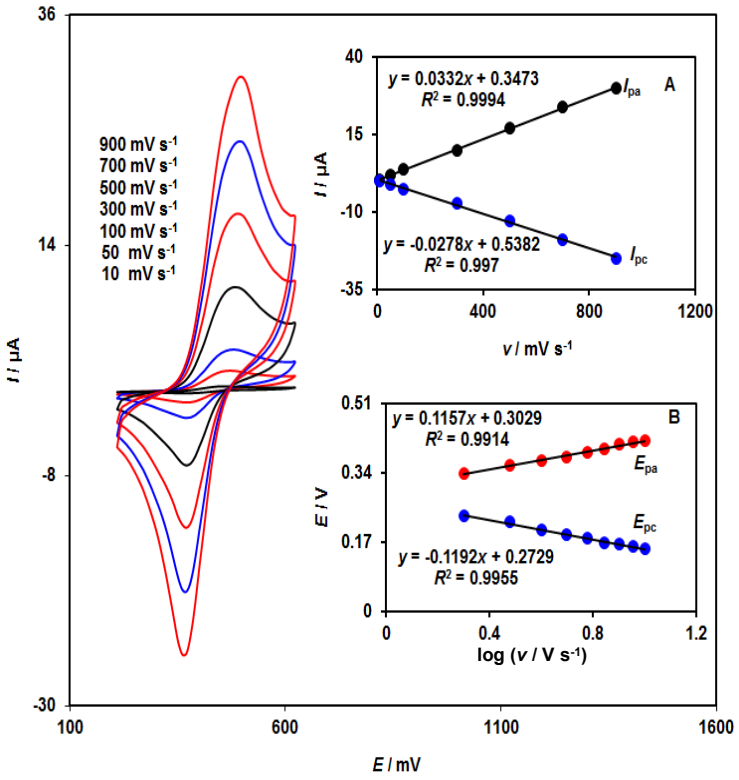

Figure 1. *CVs of Mo/NFO/CPE in PBS at different scan rates. Insets show (A)* I_{pa} *and* I_{pc} *vs. scan rate and (B)* E_{pa} *and* E_{pc} vs. *log of scan rate*

The redox pair of Mo in Mo/NFO/CPE may exhibit quasi-reversible behavior [24]. CV was also used to examine the impact of the potential scan rate (v) on characteristics of the Mo/NFO/CPE. The redox process of the molybdenum complex is not controlled by diffusion, according to plots of the anodic peak currents (I_{pa})and cathodic peak currents (I_{pc}) that were linearly dependent on v in the range of 10 to 900 mV s^{-1} (Figure 1A) [24].

According to Laviron's method [25], the shifts of E_{pa} and E_{pc} with log v can be used to determine the apparent charge transfer rate constant, k_s, and the charge transfer coefficient, α, from CV experiments. The kinetic parameters α_c and α_a (cathodic and anodic transfer coefficients, respectively) can be extracted from the slopes of the graphs in Figure 1B. For the cathodic and anodic peaks, the slope is equal to $-2.303RT/\alpha nF$ and $2.303RT/(1-\alpha)nF$, respectively. The estimated value of α is 0.5.

Also, Equation (1) can be used to determine k_s:

$$\log k_s = \alpha \log(1-\alpha) + (1-\alpha)\log\alpha - \log(RT/nFv) - \alpha(1-\alpha)nF\Delta E_p/2.3RT \quad (1)$$

where ΔE_p is $E_{pa} - E_{pc}$. and $n = 2$.

For $(1-\alpha)$ $n_\alpha = 0.5$, Equation (1) gives the value of $k_s = 22.7$ s^{-1}.

Oxidation of hydrazine at dioxo-molybdenum(VI) complex / $NiFe_2O_4$ nanoparticles modified carbon paste electrode

The pH of the aqueous solution affects the behaviour of HZN. To achieve electrocatalytic oxidation of HZN, pH adjustment of the solution appears to be required. Therefore, the electrochemical behaviour of HZN at Mo/NFO/CPE was investigated by CV at various pH values (4.0 < pH < 8.0). It was discovered that neutral conditions favour the oxidation of HZN at the Mo/NFO/CPE surface more than acidic or basic media. In the CVs of Mo/NFO/CPE, this manifests as a slow increase in the anodic peak current and a concurrent drop in the cathodic peak current. Therefore, pH 7.0 was selected as the optimal pH for Mo/NFO/CPE.

(cc) BY

In Figure 2, the CVs for electrocatalytic oxidation of HZN on unmodified CPE, NFO/CPE, Mo/CPE and Mo/NFO/CPE are shown. Notably, the peak potential for HZN oxidation on NFO/CPE and bare CPE is 930 and 970 mV, but for Mo/CPE and Mo/NFO/CPE, it is around ~325 mV.

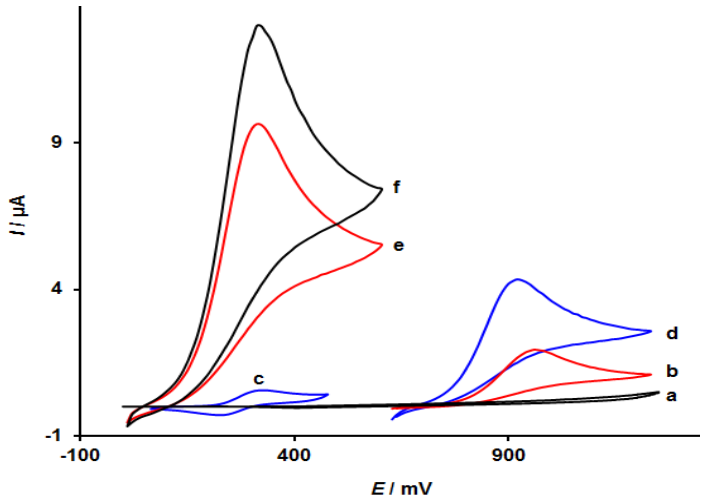

Figure 2. *CVs of (a) unmodified CPE in PBS, (b) unmodified CPE in PBS containing 50.0 µM HZN; (c) Mo/NFO/CPE in PBS; (d) NFO/CPE in PBS containing 50.0 µM HZN; (e) Mo/CPE in PBS containing 50.0 µM HZN and (f) Mo/NFO/CPE in PBS containing 50.0 µM HZN. In all cases, the scan rate is 10 mV* s^{-1}

These outcomes suggest that the molybdenum complex can act as a mediator, and the peak potential for HZN at Mo/CPE and Mo/NFO/CPE shifts by about ~605 and ~645 mV toward negative values compared with NFO/CPE and unmodified CPE. Still, Mo/NFO/CPE gives a much larger peak current for HZN than Mo/CPE does, meaning that pairing NFO with the mediator (the molybdenum complex) really boosts the electrode performance for HZN oxidation. Actually, Mo/NFO/CPE without the presence of HZN shows a redox process (Figure 2, curve c) in PBS. Yet, with 50.0 µM HZN (curve e), the behaviour points to the electrocatalytic effect of Mo/NFO/CPE [24].

Effect of scan rate

Using CV, the impact of scan rate on the oxidation of HZN was examined (Figure 3).

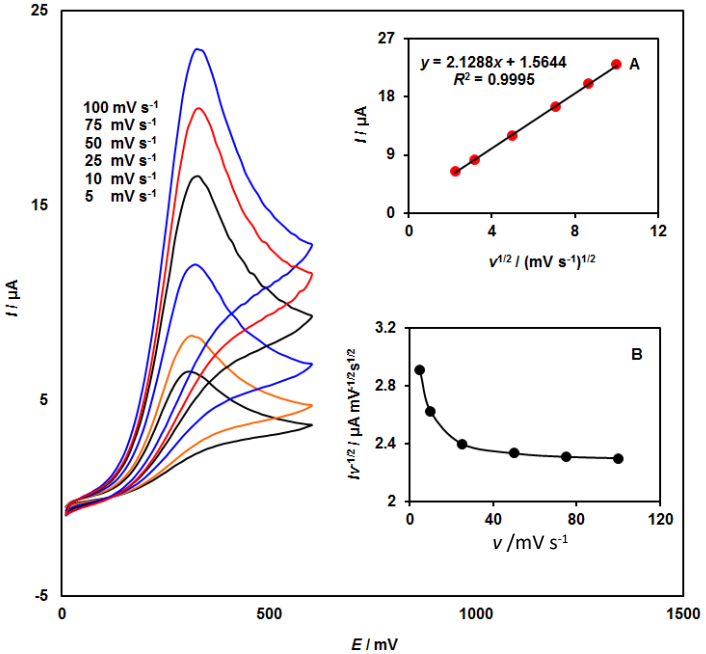

Figure 3. *CVs of 30.0 µM HZN in 0.1 M PBS, at Mo/NFO/CPE at various scan rates. Insets: (A)* I vs. $v^{1/2}$ *and (B) variation of* $I_p/v^{1/2}$ *with v*

Additionally, a plot of peak height (*I*) *vs*. the square root of scan rate ($v^{1/2}$) was shown to be linear, indicating that the process is diffusion-controlled at adequate overpotential (Figure 3A) [24]. A plot of $I/v^{1/2}$ *vs*. *v* (Figure 3B) displays the distinctive shape indicative of an EC' process [24].

Assuming *α* of 0.53, a Tafel slope of 0.1264 *V* was found (Figure 4).

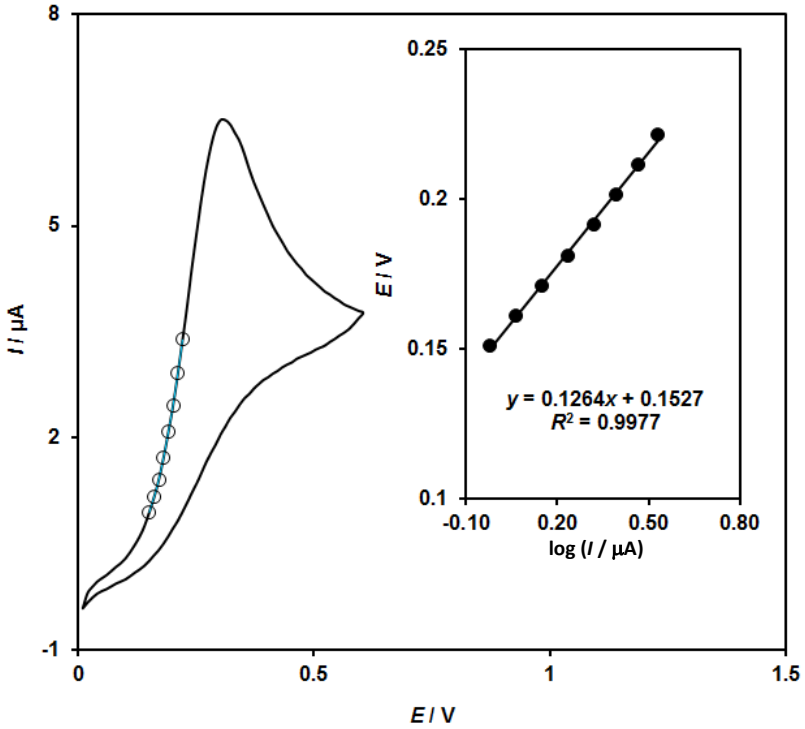

Figure 4. *CV (5 mV s^{-1}) of Mo/NFO/CPE for 30.0 µM HZN in PBS. The inset shows the Tafel plot*

Chronoamperometric studies

The working electrode potential was set to 365 mV to conduct chronoamperometric studies for various HZN concentrations at a Mo/NFO/CPE (Figure 5A). The diffusion coefficient, *D*, of HZN was calculated in chronoamperometric investigations. The best fits for various HZN concentrations were found using experimental plots of *I vs.* $t^{-1/2}$ (Figure 5B).

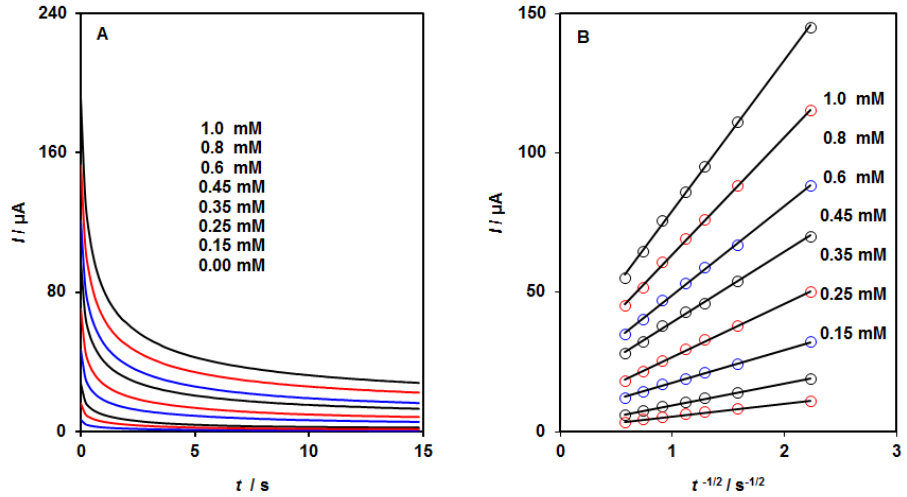

Figure 5. *(A) Chronoamperograms recorded at Mo/NFO/CPE for several HZN concentrations, (B)* I vs. $t^{-1/2}$.

The slope and the Cottrell Equation (2) [24] were then used after plotting the slopes against HZN concentration (Figure 6A):

$$I = nFAD^{1/2}C_b\pi^{-1/2}t^{-1/2} \quad (2)$$

CC BY

where C_b / mol cm^{-3} and A / cm^2 are the bulk concentration of analyte and the electrode surface area, respectively. Thus, a D = 0.000031 cm^2 s^{-1} for HZN was calculated.

According to Galus' approach [26], chronoamperometry can be used to determine the catalytic rate constant, k:

$$I_C / I_L = \pi^{1/2} \gamma^{1/2} = \pi^{1/2} (kC_b t)^{1/2} \quad (3)$$

where t /s is the duration of time, I_C is the catalytic current of HZN at the Mo/NFO/CPE and I_L is the limiting current in the absence of HZN. The k, can be determined using Equation (3), *i.e.,* using the slope of I_C/I_L versus $t^{1/2}$ (Figure 6B). The average k was determined as 18700 M^{-1} s^{-1}.

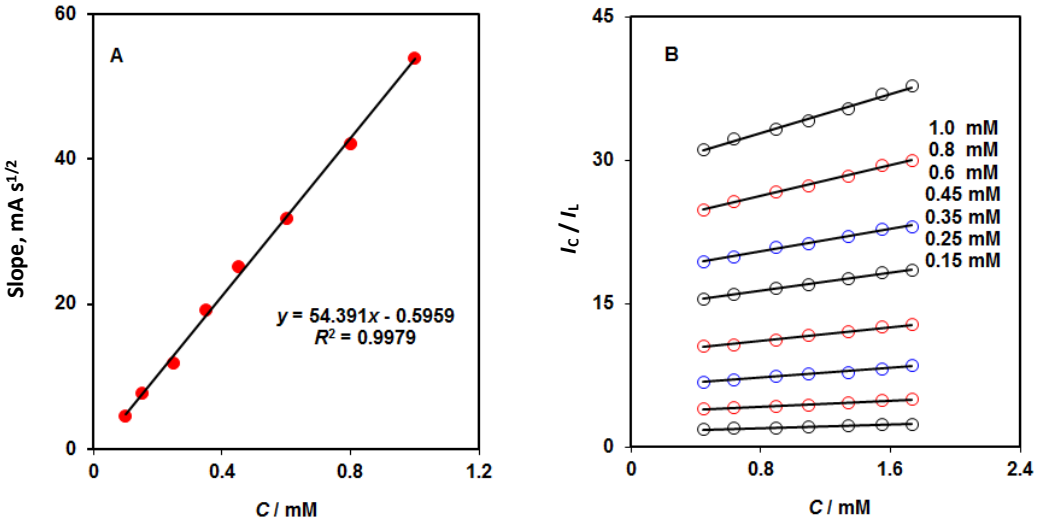

Figure 6. *(A) The slope of straight lines vs. HZN concentration. (B) The relationship of I_C/I_L with $t^{1/2}$ obtained from chronoamperograms*

Calibration plot and limit of detection

Using Mo/NFO/CPE for different concentrations of HZN, DPV tests were carried out (Figure 7). The concentration of HZN within a modified electrode was directly correlated with the peak currents of HZN at its surface in the ranges 0.1 to 50 µM (Figure 7A) and 50 to 350 µM (Figure 7B) in the DPV, with slopes of 0.2374 and 0.1017 µA µM^{-1}. The detection limit (3σ) was 0.07 µM.

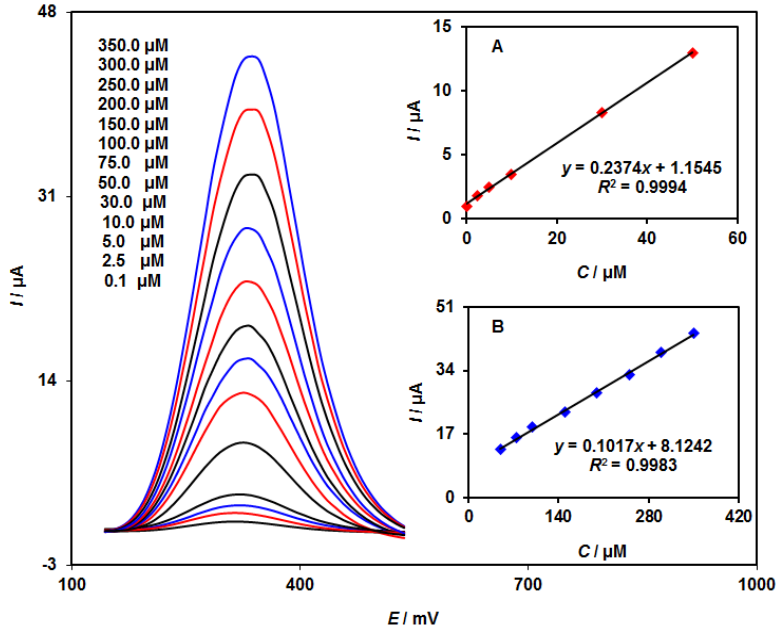

Figure 7. *DPVs of Mo/NFO/CPE in PBS containing assorted HZN levels. Insets show electrocatalytic peak current* vs. *HZN concentration: (A) 0.1 to 50.0 µM and (B) 50.0 to 350.0 µM*

Analysing the real samples

The normal addition procedure was used to measure HZN in tap water and urine samples. The obtained results are shown in Table 1. Furthermore, we observed extremely strong HZN recoveries, so reproducible results were established based on the mean RSD.

Table 1. *Determination of HZN in real samples using Mo/NFO/CPE (*n *= 5)*

Sample	Amount, μM		Recovery, %	RSD, %
	Added	Found		
Urine	5.5	5.6	101.8	3.2
	7.5	7.4	98.7	2.8
	9.5	9.8	103.2	2.3
	11.5	11.2	97.4	1.8
Tap water	4.5	4.4	97.8	2.9
	6.5	6.8	104.6	3.1
	8.5	8.4	98.8	2.0
	10.5	10.6	100.9	2.6

Conclusion

The findings showed that the molybdenum complex and $NiFe_2O_4$ nanoparticle-modified carbon paste electrode (Mo/NFO/CPE) promote HZN oxidation in a neutral environment by shifting the peak potential of HZN from 0.900 V observed for pure CPE to 0.325 V for Mo/NFO/CPE. On Mo/NFO/CPE, a notable electrochemical reaction to trace HZN was observed. This approach demonstrated a lower detection limit and a larger linear range when compared to the previously described HZN oxidation-based HZN sensor. Additionally, HZN was determined using this modified electrode. In actual samples, this sensor was effective for determining HZN.

References

[1] Z. Zhang, L. Luo, J. Liu, H. Wen, Z. Huang, W. Peng, Y. Liu, Electrodeposition-driven engineering of Ni-Fe alloy Electrocatalysts: Synergistic electronic modulation for high-performance hydrazine electrooxidation and fuel cell integration, *Journal of Power Sources* **655** (2025) 237955. https://doi.org/10.1016/j.jpowsour.2025.237955

[2] Q. Zhang, J. Zhang, G. Li, J. Yu, C. Shu, Y. Wang, W. Wang, P. Xiao, pH-dependent mechanism of hydrazine oxidation on hematite-based photoanode, *Journal of Colloid and Interface Science* **722** (2026) 140908. https://doi.org/10.1016/j.jcis.2026.140908

[3] R. Ma, X. Ma, H. Wang, X. Zhang, Y. Fang, M. Jiao, Z. Zhou, Bifunctional electrocatalysis of hydrazine oxidation and hydrogen evolution reactions on 2D CoX (X= P, S, As, Se): Insights from DFT calculations, *Chinese Journal of Catalysis* **82** (2026) 115-124. https://doi.org/10.1016/S1872-2067(25)64884-4

[4] A. N. Koreshkova, V. Gupta, A. Peristyy, P. N. Nesterenko, T. Rodemann, B. Paull, Ion chromatographic determination of hydrazine in excess ammonia for monitoring graphene oxide reduction reaction, *Talanta* **205** (2019) 120081. https://doi.org/10.1016/j.talanta.2019.06.081

[5] S. N. Tandel, A. G. Deshmukh, B. U. Rana, P. N. Patel, Studies of novel benzofuran based chalcone scaffolds: A dual spectroscopic approach as selective hydrazine sensor, *Chemical Physics Letters* **817** (2023) 140426. https://doi.org/10.1016/j.cplett.2023.140426

[6] C. Rajkumar, V. Balakumar, S. Vignesh, K. Ahmad, S. Selvarajan, W. Y. Chung, T. H. Oh, Advanced Bi_2O_3/ZrO_2/PVA nanocomposite electrode for sensitive and selective hydrazine detection, *Colloids and Surfaces A* **732** (2025) 139217. https://doi.org/10.1016/j.colsurfa.2025.139217

(cc) BY

[7] K. Ahmad, H. Kim, A brief overview of electrode materials for hydrazine sensors and dye-sensitized solar cells, *Microchemical Journal* **186** (2023) 108317. https://doi.org/10.1016/j.microc.2022.108317
[8] M. Singh, S. R. Bhardiya, A. Rai, Rai, V.K., Graphene-based nanomaterials for electrochemical sensing of hydrazine: a short review, *Current Analytical Chemistry* **19** (2023) 27-37. https://doi.org/10.2174/1573411018666220421104413
[9] R. D. Crapnell, C. E., Banks, Electroanalytical overview: the electroanalytical sensing of hydrazine, *Sensors & Diagnostics* **1** (2022) 71-86. https://doi.org/10.1039/d1sd00006c
[10] V. K. Gupta, R. Jain, K. Radhapyari, N. Jadon, S. Agarwal, Voltammetric techniques for the assay of pharmaceuticals—a review, *Analytical Biochemistry* **408** (2011) 179. https://doi.org/10.1016/j.ab.2010.09.027
[11] A. Sinha, X. Lu, L. Wu, D. Tan, Y. Li, J. Chen, R. Jain, Voltammetric sensing of biomolecules at carbon based electrode interfaces, *TrAC Trends in Analytical Chemistry* **98** (2018) 174-189. https://doi.org/10.1016/j.trac.2017.11.010
[12] S. G. Meirinho, L. G. Dias, A. M. Peres, L. R. Rodrigues, Voltammetric aptasensors for protein disease biomarkers detection, *Biotechnology Advances* **34** (2016) 941-953. https://doi.org/10.1016/j.biotechadv.2016.05.006
[13] P. Devi, R. Jain, A. Thakur, M. Kumar, N. K. Labhsetwar, M. Nayak, P. Kumar, A systematic review and meta-analysis of voltammetric and optical techniques for inorganic selenium determination in water, *TrAC Trends in Analytical Chemistry* **95** (2017) 69-85. https://doi.org/10.1016/j.trac.2017.07.012
[14] M. A. El Mhammedi, M. Bakasse, A. Chtaini, Electrochemical studies and square wave voltammetry of paraquat at natural phosphate modified carbon paste electrode, *Journal of Hazardous Materials* **145** (2007) 1-7. https://doi.org/10.1016/j.jhazmat.2007.02.054
[15] F. Valentini, V. Biagiotti, C. Lete, G. Palleschi, J. Wang, The electrochemical detection of ammonia in drinking water based on multi-walled carbon nanotube/copper nanoparticle composite paste electrodes, *Sensors and Actuators B* **128** (2007) 326-333. https://doi.org/10.1016/j.snb.2007.06.010
[16] [16] S. A. Zaidi, Graphene: a comprehensive review on its utilization in carbon paste electrodes for improved sensor performances, *International Journal of Electrochemical Science* **8** (2013) 11337-11355. https://doi.org/10.1016/S1452-3981(23)13189-0
[17] M. Achache, S. El Boumlasy, D. Bouchta, M. Choukairi, Development and applications of carbon paste and Sonogel-Carbon electrodes modified with nanomaterials: Perspectives in pharmaceutical, biological, environmental and food analysis, *TrAC Trends in Analytical Chemistry* **194** (2025) 118502. https://doi.org/10.1016/j.trac.2025.118502
[18] K. M. Elgendy, M. Z. Saad, A. F. Osman, Manganese-ciprofloxacin nanocomposite-modified carbon paste electrode for potentiometric determination of moxifloxacin, norfloxacin, and levofloxacin, *Next Material* **12** (2026) 102435. https://doi.org/10.1016/j.nxmate.2026.102435
[19] Y. Zhang, Y. Y. Zhang, C. E. Li, X. H. Yan, S. Hu, R. B. Yin, Y. F. Wei, K. Z. Gao, H. L. Gao, Research progress of $NiFe_2O_4$ electrode materials in supercapacitors: Preparation, modification, structural regulation, and future challenges, *Coordination Chemistry Reviews* **19** (2024) 216103. https://doi.org/10.1016/j.ccr.2024.216103
[20] A. A. Kumbhar, S. S. Bachankar, V. C. Lokhande, C. Kim, T. Ji, Recent innovations in ferrite-based materials for asymmetric supercapacitors, *Journal of Solid State Electrochemistry* **30** (2026) 519-566. https://doi.org/10.1007/s10008-025-06398-8
[21] K. Ahmad, S. Suganthi, S. Vignesh, T. H. Oh, Molybdenum oxide based electrode materials for electrochemical sensing applications: Recent progress in electrode modifiers, *Talanta* **302** (2026) 129366. https://doi.org/10.1016/j.talanta.2026.129366

[22] Y. Wang, Z. Li, J. Hu, L. Fang, Boosting alkaline nitrate reduction to ammonia via molybdenum-mediated hydrogenation on CuO nanoarrays, *Chemical Communications* **62** (2026) 11601-11604. https://doi.org/10.1039/d6cc01545j
[23] I. Sheikhshoaie, A. Rezaeifard, N. Monadi, S. Kaafi, A novel tridentate Schiff base dioxo-molybdenum (VI) complex: Synthesis, crystal structure and catalytic performance in green oxidation of sulfides by urea hydrogen peroxide, *Polyhedron* **28** (2009) 733-738. https://doi.org/10.1016/j.poly.2008.12.044
[24] A. J. Bard, L. R. Faulkner, H.S. White, *Electrochemical Methods: Fundamentals and Applications, 3rd Edition,* John Wiley & Sons, 2022. ISBN: 978-1-119-33405-7
[25] E. Laviron, General expression of the linear potential sweep voltammogram in the case of diffusionless electrochemical systems, *Journal of Electroanalytical Chemistry and Interfacial Electrochemistry* **101** (1979) 19-28. https://doi.org/10.1016/S0022-0728(79)80075-3
[26] Z. Galus, Fundamentals of Electrochemical Analysis, Ellis Horwood, New York, 1976. ISBN: 978-0-470-15080-1

©2026 by the authors; licensee IAPC, Zagreb, Croatia. This article is an open-access article distributed under the terms and conditions of the Creative Commons Attribution license (http://creativecommons.org/licenses/by/4.0/)